International Journal of Nanoelectronics and Materials
Volume 16 (Special Issue) December 2023 [371-383]

Optimization of Graphene infused Natural Rubber Sensing Film and Polydimethylsiloxane for Flexible Pressure Sensor

Vishnukumar Rajandran[1], Ab Rahman Marlinda[1,*], Azim Danial Azam[1], Md. Shalauddin[1], A. A Saifizul[2,*], Syed Muhammad Hafiz[3], Shafarina Azlinda[3]

[1]Nanotechnology and Catalysis Research Centre (NANOCAT), Universiti Malaya, Malaysia
[2]Mechanical Engineering Department, Faculty of Engineering, Universiti Malaya, Malaysia
[3]Centre for Semiconductor & Thin Film Research, Advanced Materials & Semiconductor Technology Department, MIMOS Berhad, Malaysia

ABSTRACT

A flexible and stretchable pressure sensor offers significant benefits in human-computer interaction, healthcare, and tactile sensing in robots. We present a novel study optimising Polydimethylsiloxane (PDMS) and graphene-infused unvulcanised natural rubber sensing film to increase sensor sensitivity and dielectric permittivity. By optimising the PDMS thickness uniformity, NR-G film's impedance and capacitance-pressure loading response, it is possible to enhance the pressure sensor's sensitivity across a wide pressure range, covering human finger motion. With our synthesized homogenous 5wt% of NRG composite, a capacitance value of 193pF was achieved when applying pressure of 150 kPa at a frequency of 0.5 Hz. Excellent sensitivity and dielectric permittivity of 0.020 kPa^{-1} and 109.1, respectively, which is ~ 6.5 folds higher than pure NR. PDMS thickness of 300µm with ±3% uniformity was achieved using 90s spin time and 200rpm spin speed. This optimisation of sensing material and substrate is important in developing wearable sensors having applications in soft robotics, health monitoring electronics, and soft human-machine interfaces.

Keywords: Natural rubber, graphene nanoplatelet, pressure sensor, impedance spectroscopy, capacitance

1. INTRODUCTION

Conductive polymeric composites (CPC) combine a unique attribute for polymeric materials—the capacity to display electrical conductivity—with traditional properties of polymeric materials, such as cheap cost, processability, and low density. This conductivity can frequently be achieved by adding conductive fillers to a composition and a conductive phase. Due to its high deformability and flexibility without sacrificing other mechanical qualities, conductive rubber composites (CRC) are rising, especially in multiple load cyclic activities. Applications for CPCs and CRCs can be found in a wide range of products, including supercapacitors[1-3], biochemical sensors[4,5], and flexible printed electronics[6,7].

Rubber can be modified to have conductive qualities by introducing carbon-based compounds such as carbon black (CB)[8,9], carbon nanotubes (CNT)[10,11], graphene[12], and its derivatives. Because of its chemical and physical qualities, as well as its strong interaction with natural rubber (NR), carbon black has traditionally been the most commonly employed filler in NR compounds. Furthermore, the employment of CB in the development of CPCs has been widely discussed. Carbon nanotubes have a high potential for usage in elastomeric materials due to their unique mechanical, magnetic, and electrical characteristics. Furthermore, they have a greater aspect ratio than C, facilitating the build-up of a percolated network and promotes electron flow. As a result, developing hybrid composites with fillers of varying forms and aspect ratios may be

* Corresponding authors: marlinda@um.edu.my; saifizul@um.edu.my

an interesting technique for improving CRCs by enhancing network contact points between fillers. The processing method is critical in this line of work because the dispersion of the fillers determines what features are transferred from the nanoparticles to the matrix. Then, the ultrasound dispersion method in latex is used to break the van der Waals connection between fillers in a liquid media, increasing the filler network morphology and electrical characteristics.

The key challenges to address while fabricating sensors based on CRCs are capacitive and resistive properties study. Piezo-resistivity is defined in this context by structural deformations, which result in the changes of material resistivity. Piezo-resistivity analysis is frequently used to depict sensors based on CRCs. It can be improved by varying the conductive additives' concentration, morphology, and interactions with the polymer matrix. Metal-based sensors offer great sensitivity but degrade over time owing to deformation cycles and have a poor deformation capacity (~5%). One of the current issues is balancing the two normally opposing traits of high sensitivity and stretchability. In this approach, the creation of piezoresistive elastomers is attractive because they are easier to obtain, less expensive, have higher sensitivity, very high strain sensitivity (ΔR/R0), and provide long-lasting and stable performance after service.

Piezo-resistivity measurement can be characterised using electrochemical impedance spectroscopy (EIS) with ease because it is a real-time, non-destructive method that rapidly provides information about complex conduction mechanisms and dielectric properties, while conventional resistivity characterisation generally provides resistivity only. Therefore, piezo-impedance analysis has been used to evaluate both resistive and capacitive effects and has the advantage of being directly measured by an EIS analyzer since piezo-resistivity needs posterior data treatment using an equivalent electrical circuit whose construction depends on the polymer, fillers, interfaces, and transport mechanisms involved. For example. Lee et al. [13] prepared a compressive resistance material based on 2D MXene ($Ti_3C_2T_x$) with a 1D nitrogen-doped graphene nanoribbon (N-MX/GNR) that was then coated onto the surface of a 3D open-network porous latex rubber by a dip coating process and found that able to achieve high sensitivity and low detection limit (3Pa). In order to enhance the flexibility and strength of a 3D graphene skeleton, one common strategy is to fabricate a sensor with outstanding stability and excellent durability by polymers or elastomers into the graphene materials themselves. However, to the best of our knowledge, there is no research based on unvulcanised natural rubber filled graphene nanocomposites that has been studied by impedance spectroscopy in capacitive sensing experiments.

The paper aimed to prepare and optimise the unvulcanised natural rubber nanocomposites for piezocapacitance applications with different weight content of conductive filler using the ultrasonication-assisted solution blending method. In this study, the weight content of graphene in natural rubber and thickness of PDMS are optimised to provide high capacitive response, signal sensitivity and film uniformity for capacitive pressure sensor application. For this purpose, the LCR meter and DMA machine were chosen to evaluate the changes in piezo-impedance properties due to the addition of graphene and to assess the electrical properties of the fabricated nanocomposites under static and cyclic pressure loading. The results show that the nanocomposites have great potential for applications as pressure sensitive materials and piezo-impedance, primarily capacitive-based sensors.

2. MATERIAL AND METHODS

2.1 NR-GNP Composite Synthesis

Natural rubber (CV-60 dry rubber) was procured from the Malaysia Rubber Board, Malaysia. While, graphene nanoplatelet (GNP) was purchased from Nanografi NanoTechnology, Turkey. Toluene was obtained from Merck (Germany). The reagents and solvents used are of analytical grade and need no further purification before use. The natural rubber infused graphene (NRG) was carefully synthesised following the ultrasonication-assisted solution blending method, as reported by Marlinda et al. [14]. Initially, dried CV-60 natural rubber (NR) was sliced into small pieces to increase its surface area before being dissolved in toluene. For the preparation of NR solution with 5% and 10% total solid content (TSC), 5 g and 10 g of NR was added to 100 mL of toluene, respectively. The NR was slowly added into the toluene under continuous stirring to homogenize the NR solution. Next, to prepare the NRG composite, the required volume of the NR solution was then blended with the required amount of GNP as shown in Table 1, using a top-down stirring method with a generic handheld electric drill for 1 h to disperse the NRG. The mixture was then sonicated for 1 hour with 100 Watts at 100% amplitude using a UP200Ht Ultrasonic Processor from Hielscher. The pure NR and NRG with 1, 2 and 5 wt% were synthesised as shown in Figure 1A. Finally, the solution was then cast in a mold and dried in an oven overnight at 60 °C to form films as shown in Figure 1B. The dried films performed morphology and electrical characterisation to evaluate the performance and stability of composites.

Table 1 Formulation for NRG composite

	NR 10% TSC 0 wt.% GNP	**NR 10% TSC 1 wt.% GNP**	**NR 5% TSC 2 wt.% GNP**	**NR 10% TSC 2 wt.% GNP**	**NR 10% TSC 5 wt.% GNP**
Volume of NR Solution (mL)	25	25	25	25	25
Weight of GNP (mg)	0	25	25	50	125

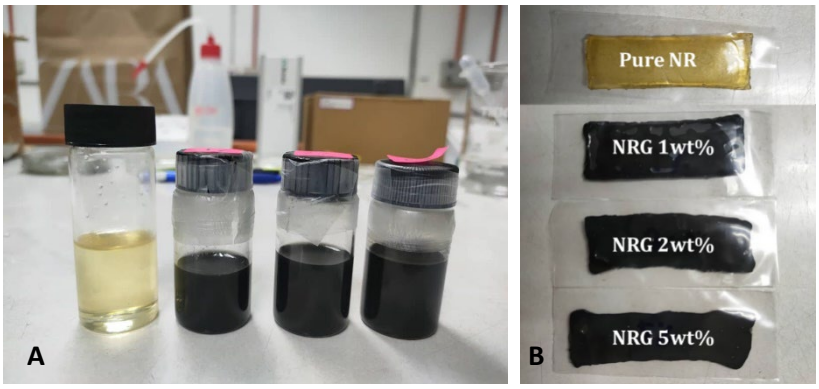

Figure 1. (A) (Left to Right) Images of pure unvulcanised natural rubber solution, Natural rubber infused graphene (NRG) solution with 1 wt%, 2 wt% and 5 wt% filler. (B) Dried NR and NRG film composites.

2.2 NR-GNP Composite Characterisation

Scanning electron microscopy (SEM, FEI Sirion-200) observed the morphological structure of nanocomposites. The impedance characteristics were recorded using a HP4192A LCR meter in the range of 10 Hz-10 MHz at a 50 mV oscillator level. A dynamic mechanical analyser (DMA, ElectroForce 3200, TA instruments, Minnesota 55344 USA) was utilised to supply the

compressive force to the nanocomposite. The rubber composite was connected with the DMA clamp to evaluate the electrical performance. For the compression test, the copper foil was used as top and bottom electrode of the NR-GNP sample [15]. The sample was clamped using clips on copper foils. The sample was cut to have an area and thickness of 4 cm^2 and 2 mm, respectively. The SEM, EDX, Impedance and capacitance results of NR-GNP are described in Subsections 3.1 to 3.3.

2.3 PDMS fabrication

The PDMS prepolymer and curing agent were acquired from standard commercial (Sylgard 184, Dow Corning) and used directly without further purification. PDMS prepolymer and curing agent were mixed at a ratio of 10:1 and mechanically stirred for 10 min at room temperature. The mixture was then cast on a clean glass slide by spin coating for reproducible thickness. Varying spin times and spin speeds were investigated to achieve the optimum uniformity in thickness. The results are described in Subsection 3.4.

3. RESULTS AND DISCUSSION

3.1 Microstructure and Interfacial Interaction of NR-GNP Nanocomposite

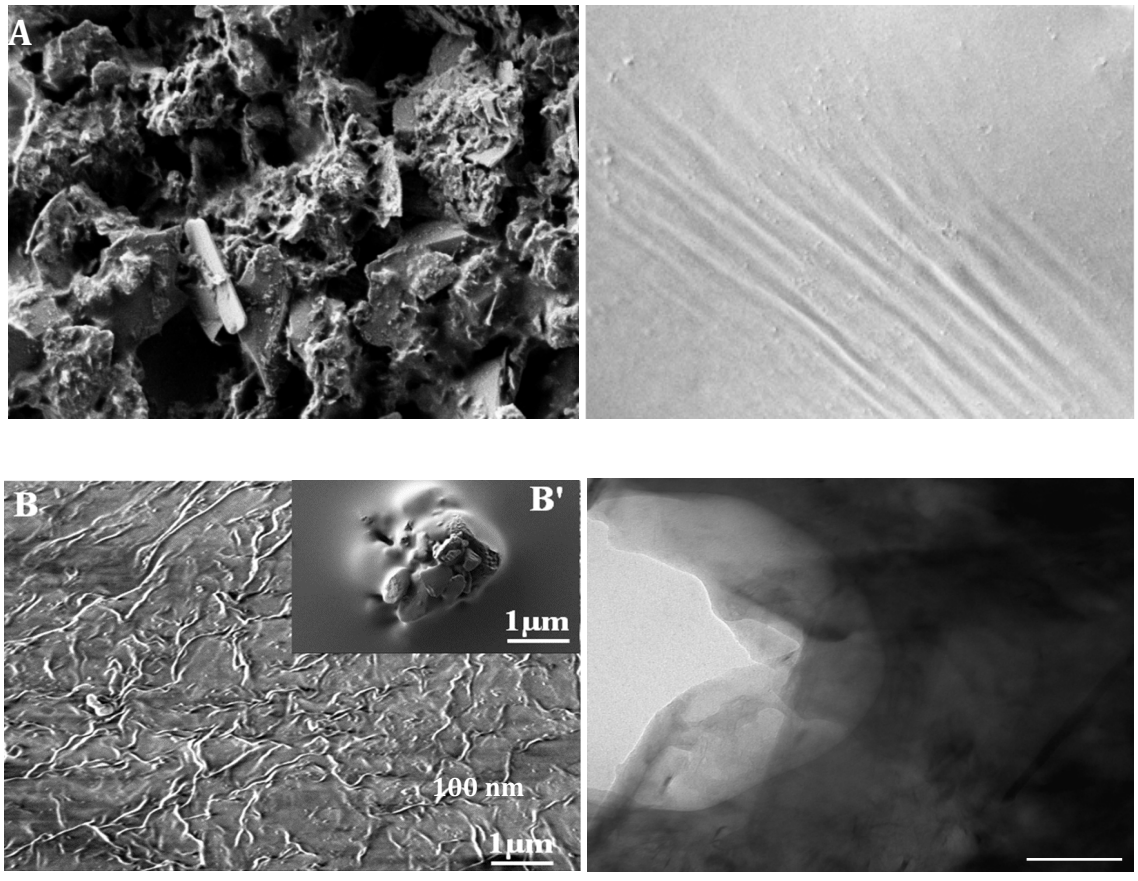

Figure 2. FESEM image of (A) graphene nanoplatelet, (B-B') graphene nanoplatelet and natural rubber composite sample synthesized by an ultrasonication-assisted solution blending method [14] and (C) pure natural rubber sample. (D) TEM image of graphene nanoplatelet and natural rubber composite sample.

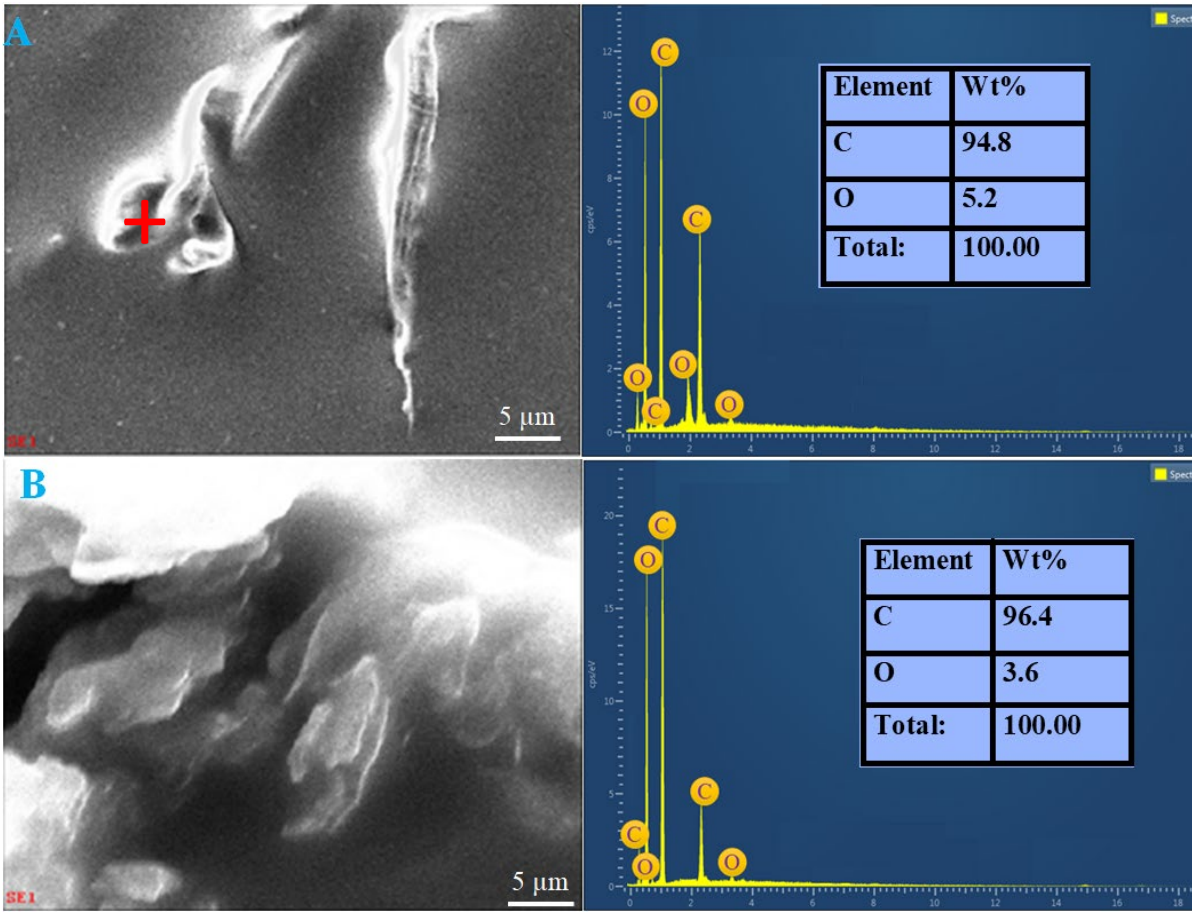

Figure 3. EDX analysis for 5% TSC and 2% GNP (A), and 10% TSC 2% GNP (B).

Figure 2A shows the FESEM images of GNP. In contrast, Figure 2C shows the FESEM image of the pure NR and Figures 2B, 2B' and 2d show NR-infused GNP nanocomposite. It can be seen that pure NR has a flat and smooth surface. NR with GNP nanocomposite, however, presents a rough surface compared with NR. This rough surface is attributed due to the good adhesion of the GNP to the layer of rubber. The relatively well attachment and high homogeneity result from the consistent ultrasonication carried out during blending for long hours, whereby the GNP has successfully infused and blended well in the NR matrix. From FESEM image (Figure 2B') it is clearly observed that, the surface of GNP is deposited on the surface of NR matrix. Due to the surface attachment of GNP and NR, a distinct morphology is observed and presume that there is interfacial interaction between GNP and NR which is further proved by the capacitive and impedance analysis. These findings indicate the presence of strong interfacial interactions between the rubber chain macromolecules and the graphene nanofillers. The homogenous polymer-filler dispersion and strong interfacial interaction are desirable for GNP to enhance its reinforcing performance in the NR matrix, resulting in a potential increase in the mechanical performance of NR-GNP nanocomposites. The EDX results (Figure 3) clearly show that the scanned area (red + sign marking) consisted of graphene. The major element presented in the rubber film composite was carbon element, with 94.8 weight % and 96.4 weight % for rubber, with 5% TSC and 10% TSC, respectively. The reason for that is the main polymer part is cis-1, 4-polyisoprene(-C_5-H_7-) units and graphene atoms that mainly consist of carbon elements. The C/O ratio in rubber composite is higher in 10% TSC compared to 5% TSC due to more rubber content present in the sample.

3.2 Impedance Response of NR-GNP Nanocomposite

Pure natural rubber, graphene, and rubber nanocomposite with 1wt% and 2wt%, as shown in Figure 4(left), were prepared and characterised using an LCR meter to analyse their electrical property. Figure 4(right) shows the setup where the mounting places the sample between two metal clamps, which act as electrodes to allow an electric field to pass through the NRG film. This setup represents an ideal capacitor; hence, it can be represented by an idealized equivalent circuit comprised of resistors (R) and capacitors (C) (Figure 5)[16].

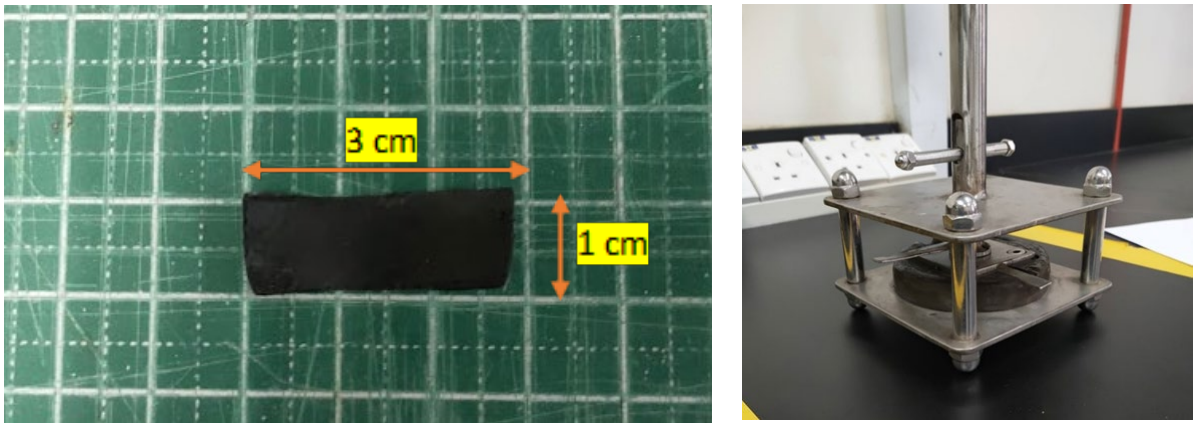

Figure 4. (Left) Natural rubber infused graphene sample was prepared with dimensions 3cm by 1cm (length and width). (Right) A mounting used to clamp the rubber samples and connected to LCR meter to perform the impedance measurement.

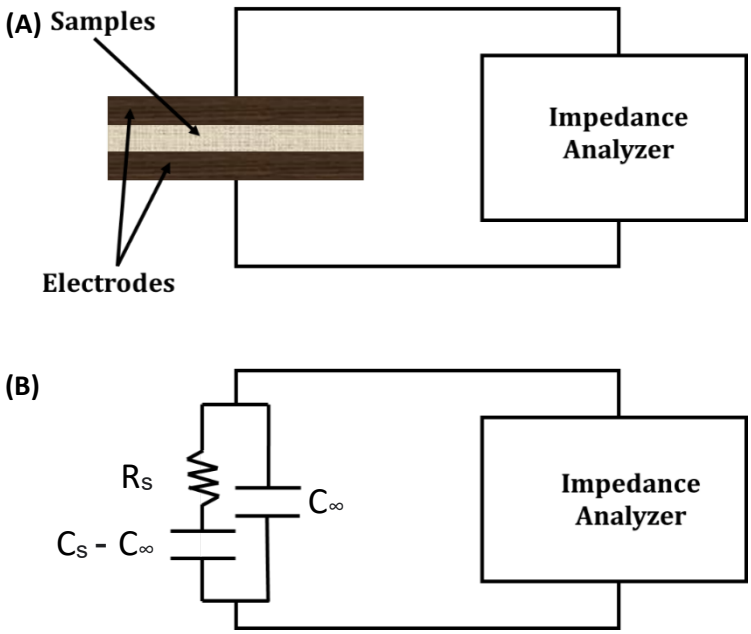

Figure 5. Equivalent circuit (B) to represent the NRG film placed between two metal electrodes (A) [16].

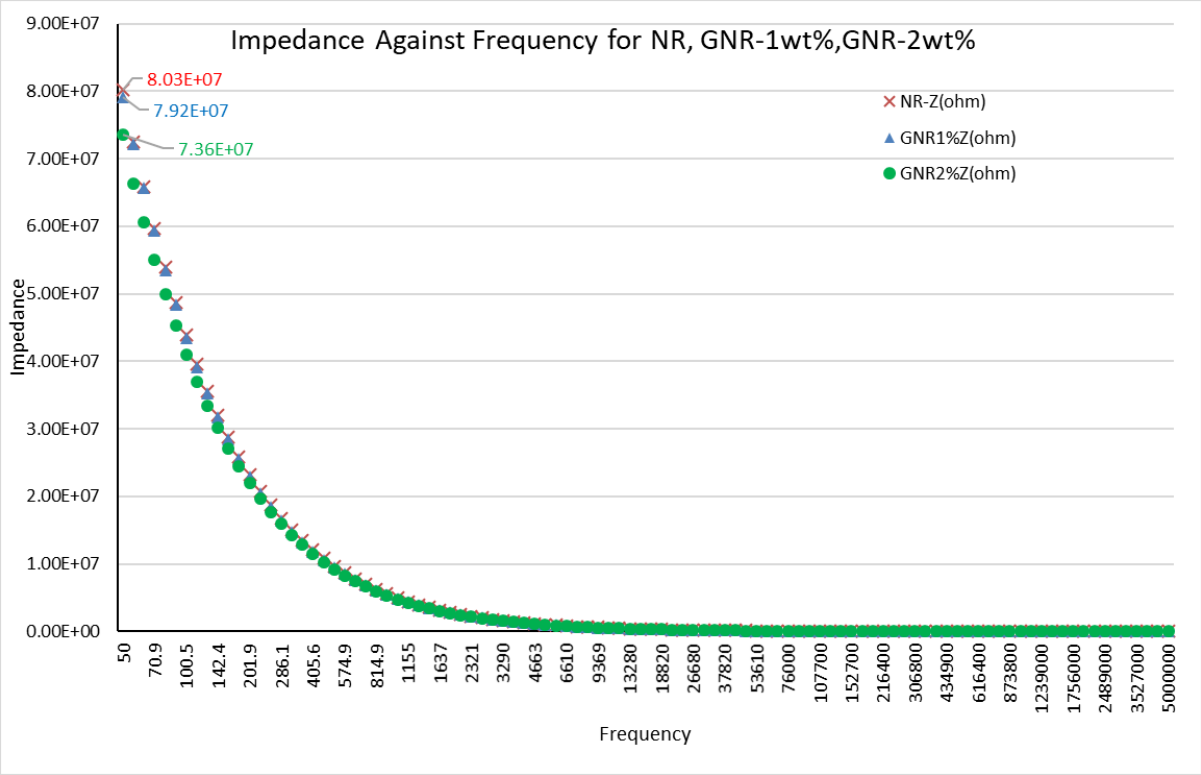

Figure 6. Impedance measurement of pure natural rubber, rubber with 1wt. % graphene, and rubber with 2wt. % graphene at varying frequency.

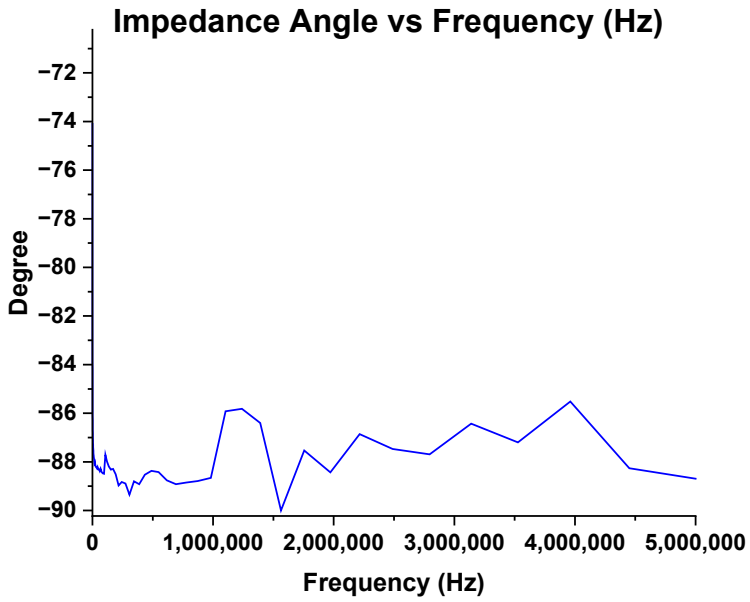

Figure 7. Impedance angle versus frequency measured using LCR meter.

Figure 6 shows the impedance measurement, which accounts for the frequency-dependent electrical resistance of the rubber composite. At the frequency of 50 Hz, 2% GNP recorded the lowest impedance of 74 MΩ whereas pure NR recorded the highest impedance of 80 MΩ (The incorporation of graphene has reduced the impedance). The 2% GNP exhibits lower impedance than 1% GNP in NR with 74 MΩ and 79 MΩ at 50 Hz, respectively. Clearly, the impedance reduces

as graphene concentration increases. The incorporation of graphene has improved the electrical properties of natural rubber. As the graphene content increases in the rubber matrix, the connected network of graphene increases, resulting in lower impedance in the nanocomposite. The impedance measured consists of a real part (resistance) and an imaginary part (reactance), and the phase angle can be computed as $\tan^{-1}$ (reactance/resistance), which explains the phase shift between voltage and current signals [16]. In Figure 7, the measured phase angle (degrees) gives a horizontal line almost close to -90°, hence can be regarded as a pure electric capacitor. The phase angle of NRG sample is measured in the range of -86° to -89° when an AC field is applied. The phase angle values of sample has small values of phase shift, δ. Therefore, an ideal capacitor phase shift of -90° is not possible due to noise in the signal. Nevertheless, the NRG composite exhibits excellent capacitive behaviour in AC signal. The capacitive effect and other parameters, such as dielectric permittivity and sensitivity, are explained in the following section.

3.3 Capacitance Response of NR-GNP Nanocomposite

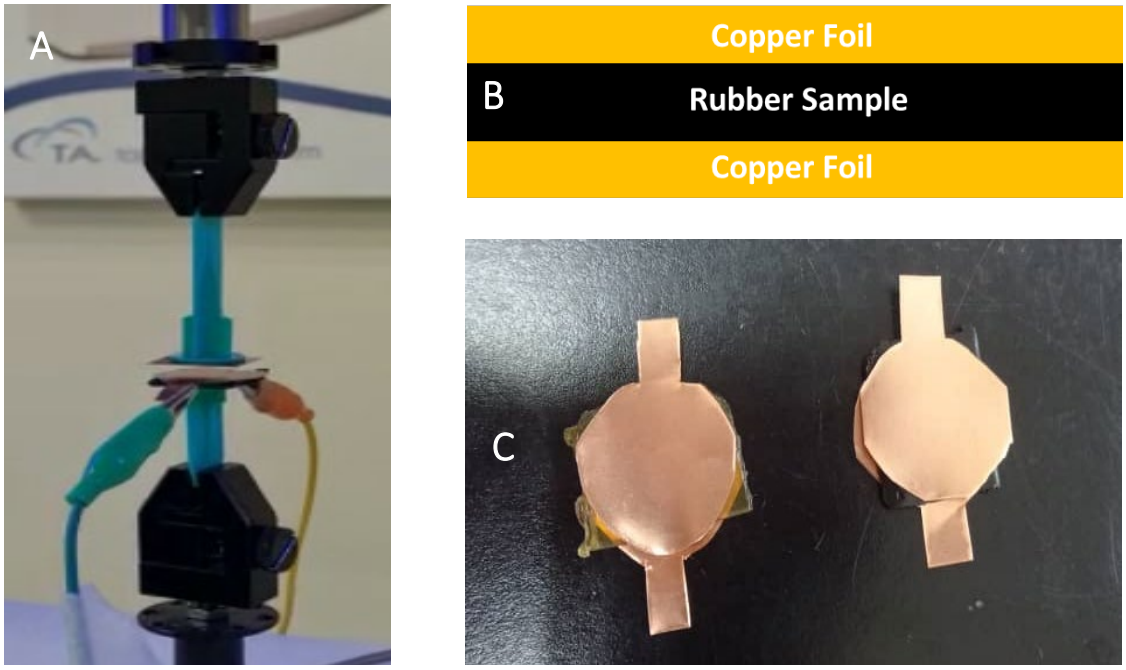

Figure 8. (A) Compressive test system with DMA clamp. (B) Side view and (C) Top view of rubber composite sample size of 2 cm by 2 cm sandwiched between copper foils prepared for compression testing.

One of the important requirements for flexible sensors was maintaining their electrical functionality during the deformation. In order to achieve that, the active sensing material has to possess both stretchability and conductivity. To assess the mechanic-electric coupling properties, the sensing performance of natural rubber infused with 2 and 5 wt% graphene content was tested by applying compressive force. To evaluate the compressive behaviour, a 3D-printed plastic bar was used to compress the surface of NRG perpendicularly for the simulation of a finger (Figure 8A). Then, the compressive test system, consisting of the DMA and the 3D printed bar, was established.

As shown in Figure 8C, the dimension of each sensing element in our current work is 2 cm by 2 cm. A calibrated digital caliper measured the thicknesses of the prepared sample. Applying the equation below, the dielectric constant of the NRG film can be calculated.

$$C = \varepsilon_r \varepsilon_0 A/d \quad (1)$$

Where C is the capacitance of the sensing element; ε_r is the relative permitivity (i.e., dielectric constant; relative permittivity ε_r of air is 1) of prepared the NRG film; ε_0 is the permivity of free space (8.854×10^{-12} Fm^{-1}); A is the area of the sensing element; and d is the distance between the top and bottom electrodes (2 mm). The samples were fabricated according to the procedure described in Section 2. The calculated and measured parameters are shown in Table 1. The calculated relative permittivity ε_r of the NRG film is ~42 to 109 (measured at 0.5 Hz). Since the sensing elements are capacitive type, the relationship between capacitance changes and applied pressure is determined. The films were tested under an applied pressure ranging from 0 to 150 kPa. The sensitivity S of this wide range is calculated using the following equation:

$$S = 1 \times \Delta C / \Delta P \times C_0 \quad (2)$$

Where C_0 is the initial capacitance, ΔC is the change in capacitance; and ΔP is the change in pressure. The sensitivity changes clearly along with graphene content in rubber. As shown in Table 1, the sensitivity increases from 0.0031 kPa^{-1} to 0.020 kPa^{-1} which is ~ 6.5 folds higher as the graphene content increases.

Table 1 Parameters of the NRG films

Sample	**A**	**B**	**C**
Graphene content (wt%)	0	2	5
Measured initial Capacitance (pF)	50.5	51.8	47.9
Max Capacitance at 150 kPa *measured at 0.5 Hz (pF)	73.9	87.9	193.2
Calculated Relative Permittivity	41.7	49.7	109.1
Sensitivity (kPa^{-1})	0.0031	0.0046	0.020

The cyclic compressive response was measured at frequency of a 0.5 Hz and subjected to a load force of 59N over time. The response is shown in Figure 9. The composite showed a stable operation and exhibited a fast response under repetitive loading/unloading cycles for different pressures. Time of response is a crucial parameter in pressure sensing that must be considered to minimise the sensor lag of response. The capacitance response increased with graphene content. The main reason is due to the increase in GNP concentration in the rubber matrix. Thus, when the NRG suspension is dried, more GNP will be closely arranged, building a denser network resulting in better conductivity and consequently improving the sensitivity.

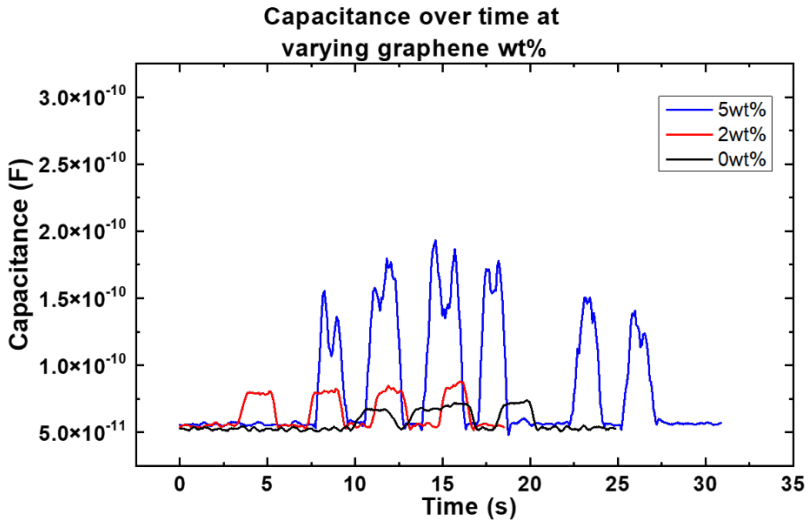

Figure 9. Cyclic response of the active sensing material natural rubber – graphene (NRG) at 0, 2 and 5 wt% of graphene content.

3.4 PDMS Fabrication

In our design, we use PDMS as a substrate; therefore, it is crucial to precisely control the thickness and uniformity of PDMS layers. PDMS was cast on a glass slide by spin coating for reproducible thickness control and cured in a drying oven. Figure 10 shows the spin-coated PDMS thickness at various spin speeds and times, respectively. The plateau of the graph in Figure 10 (inset) indicates that the thickness is independent of spin time for the range of 30 to 300 seconds. (Lee, Chang, & Yoon, 2007) The thickness of cured PDMS was able to be controlled from 300µm to 5µm by spin coating within ±9% variation. As for over 300µm in thickness, it is difficult to control the PDMS thickness by spin coating. The target was ±5% uniformity for a 300µm PDMS thickness over a 2-in glass slide, and could eventually achieve ±3% uniformity for 300µm PDMS. The thickness was measured using a laser profiler from Bruker (Dektak XTL™ Stylus Profiler). The PDMS layer acts as a flexible substrate for the pressure sensor.

.

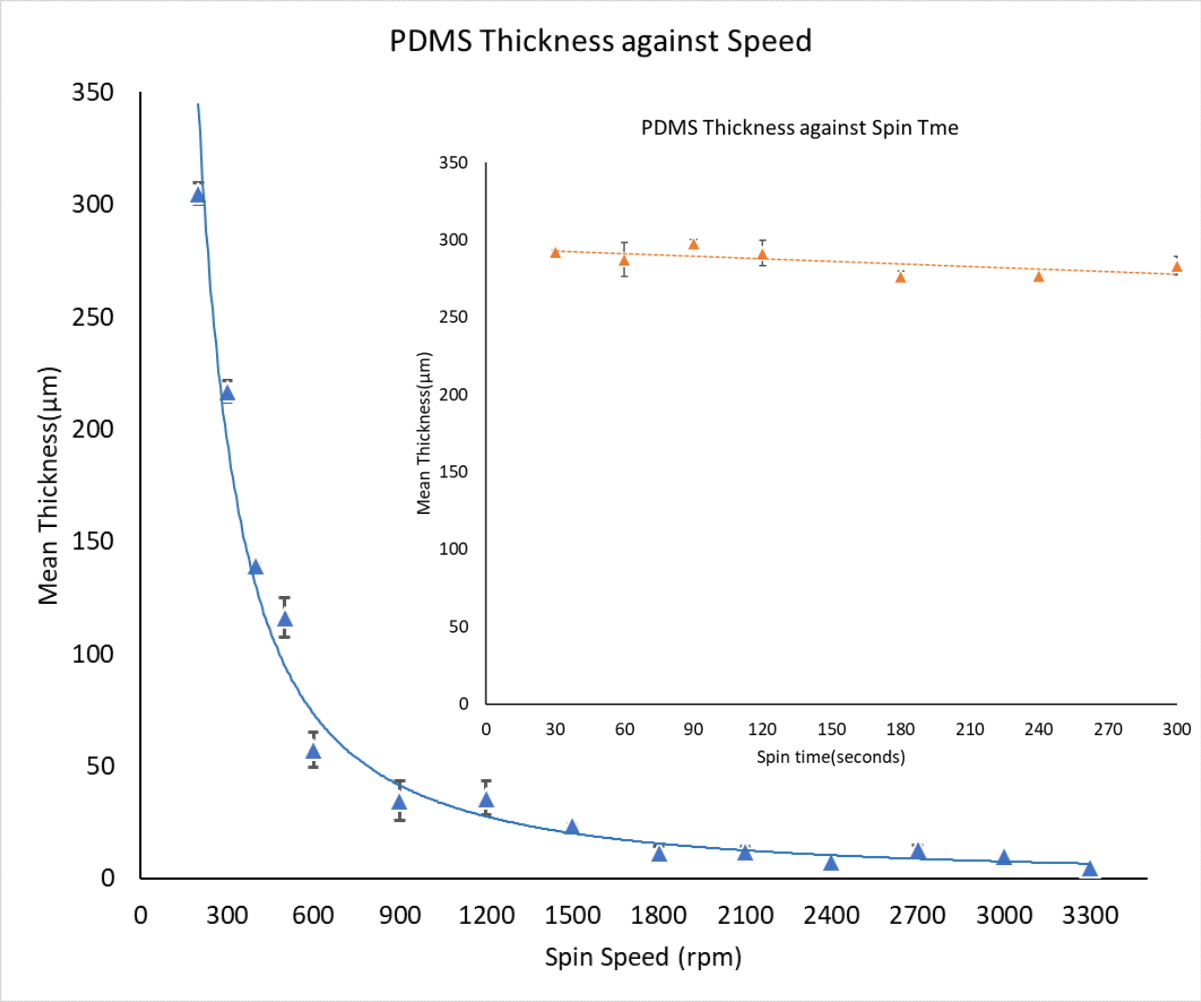

Figure 10. Thickness of spin-coated PDMS layers for different spin speed with spin time fixed at 90 s. Inset image shows thickness of spin-coated PDMS layers for different spin time with spin speed fixed at 200 rpm.

4. CONCLUSION

We have reported a cost-effective and simple technique to fabricate unvulcanised NRG composite using an ultrasonication-assisted solution blending method. Incorporating graphene, which has excellent electrical conductivity and integration of unvulcanised NR, has successfully shown a good cyclic pressure loading response. The well adhesion of the GNP to the layer of rubber, resulting in high homogeneity, is due to the consistent ultrasonication. FESEM and EDX successfully measured the homogeneous surface morphology and C/O element ratio. The impedance spectroscopy proved that the fabricated composites are capacitive, as the phase angle is close to -90°. The optimised concentration of 5 wt% NRG responded to the highest sensitivity and dielectric permittivity of 0.020 kPa^{-1} and 109.1, respectively, which is ~ 6.5 folds higher than pure NR. Also, the 5 wt% composite measured a capacitance value of 193pF when applied pressure of 150 kPa at the frequency of 0.5 Hz. The PDMS substrate is optimised to achieve a uniform thickness of 300µm with ±3% using 90s spin time and 200 rpm spin speed. The optimised spin coating parameters of PDMS and weight content percentage of graphene in NR reported in the study provides the critical building block components required for an excellent pressure sensor with great flexibility and potential use in application such as supercapacitors, biochemical sensors, and flexible printed electronics.

ACKNOWLEDGEMENTS

The authors would like to thank the Ministry of Higher Education (MoHE) Malaysia for funding this work via research grant number PRGS/1/2022/STG05/UM/02/3 (PR003-2022) and the Universiti Malaya for the funding of this research via the UM International Collaboration Grant with grant number IMG006-2023. The authors also would like to thank Mrs. Hani Afiffa Binti Mohd Hanif from the Malaysia Rubber Board for supplying the natural rubber resources and Associate Prof. Dr. Ahmad Shuhaimi Bin Abu Bakar from the Department of Physics, Faculty of Sciences, Universiti Malaya for providing the profilometer testing facilities to support this work.

REFERENCES

[1] G. A. Snook, P. Kao, and A. S. Best, "Conducting-polymer-based supercapacitor devices and electrodes," Journal of Power Sources, vol. 196, no. 1, pp. 1-12, 2011.

[2] S. Sagadevan, A. R. Marlinda, M. R. Johan, A. Umar, H. Fouad, O. Y. Alothman, U. Khaled, M. S. Akhtar, and M. M. Shahid, "Reduced graphene/nanostructured cobalt oxide nanocomposite for enhanced electrochemical performance of supercapacitor applications," Journal of Colloid and Interface Science, vol. 558, pp. 68-77, 2020.

[3] A. N. Grace, S. Venkateshalu, and S. Gnanasekar, "Carbonaceous nanocomposites for supercapattery," in Advances in Supercapacitor and Supercapattery, N. Arshid, M. Khalid, and A. N. Grace, Eds. Elsevier, 2021, pp. 93-110. ISBN 9780128198971.

[4] J. H. Oh, J. Y. Woo, S. Jo, and C.-S. Han, "Pressure-conductive rubber sensor based on liquid-metal-PDMS composite," Sensors and Actuators A: Physical, vol. 299, 111610, 2019.

[5] S. Gupta, A. Sharma, and R. S. Verma, "Polymers in biosensor devices for cardiovascular applications," Current Opinion in Biomedical Engineering, vol. 13, pp. 69-75, 2020

[6] S. M. F. Cruz, L. A. Rocha, and J. C. Viana, 'Printing Technologies on Flexible Substrates for Printed Electronics', Flexible Electronics. InTech, Jul. 25, 2018. doi: 10.5772/intechopen.76161.

[7] S. Xu, X.-L. Shi, M. Dargusch, C. Di, J. Zou, and Z.-G. Chen, "Conducting polymer-based flexible thermoelectric materials and devices: From mechanisms to applications," Progress in Materials Science, vol. 121, p. 100840, 2021.

[8] S. Podhradská, J. Prokeš, M. Omastová, and I. Chodák, "Stability of electrical properties of carbon black-filled rubbers," Journal of Applied Polymer Science, vol. 112, no. 5, pp. 2918-2924, 2009.

[9] I. Chodák, S. Podhradská, J. Jana Jarčúšková Podhradská, and J. Jurčiová, "Changes in electrical conductivity during mechanical deformation of carbon black filled elastomeric matrix," The Open Macromolecules Journal, vol. 4, no. 1, 2010.

[10] Y. Nakaramontri, C. Kummerlöwe, C. Nakason, S. Pichaiyut, S. Wisunthon, and F. Clemens, "Piezoresistive carbon-based composites for sensor applications: Effects of polarity and non-rubber components on shape recovery," Express Polymer Letters, vol. 14, pp. 970-986, 2020.

[11] T. S. Natarajan, S. B. Eshwaran, K. W. Stöckelhuber, S. Wießner, P. Pötschke, G. Heinrich, and A. Das, "Strong strain sensing performance of natural rubber nanocomposites," ACS Applied Materials and Interfaces, vol. 9, pp. 4860-4872, 2017.

[12] C. S. Boland, U. Khan, C. Backes, A. O'Neill, J. McCauley, S. Duane, R. Shanker, Y. Liu, I. Jurewicz, A. B. Dalton, and J. N. Coleman, "Sensitive, High-Strain, High-Rate Bodily Motion Sensors Based on Graphene–Rubber Composites," ACS Nano, vol. 8, no. 9, pp. 8819-8830, 2014.

[13] H. J. Lee, J. C. Yang, J. Choi, J. Kim, G. S. Lee, S. P. Sasikala, G.-H. Lee, S.-H. K. Park, H. M. Lee, J. Y. Sim, S. Park, and S. O. Kim, "Hetero-dimensional 2D Ti3C2Tx MXene and 1D graphene nanoribbon hybrids for machine learning-assisted pressure sensors," ACS Nano, vol. 15, no. 6, pp. 10347-10356, 2021

[14] A. R. Marlinda, N. H. Kamaruddin, A. W. Fadilah, M. Said, N. A. Hamizi, and M. R. Johan, "Simple dispersion of graphene incorporated rubber composite for resistive pressure sensor application," Polymer Engineering & Science, vol. 61, no. 5, pp. 1476-1484, 2021.
[15] T. Hu, S. Xuan, L. Ding, and X. Gong, "Liquid metal circuit based magnetoresistive strain sensor with discriminating magnetic and mechanical sensitivity," Sensors and Actuators B: Chemical, vol. 314, 128095, 2020.
[16] W. H. Hunter Woodward, "Broadband Dielectric Spectroscopy—A Practical Guide," in Broadband Dielectric Spectroscopy: A Modern Analytical Technique, chap. 1, pp. 3-59.